

# Can the exciton–polariton regime be defined by its quantum properties?

D. G. Suárez-Forero,<sup>1</sup> G. Cipagauta,<sup>1</sup> H. Vinck-Posada,<sup>1,\*</sup> K. M. Fonseca-Romero,<sup>1</sup> and B. A. Rodríguez<sup>2</sup>

<sup>1</sup>*Universidad Nacional de Colombia - Bogotá, Facultad de Ciencias,  
Departamento de Física, Grupo de Óptica e Información Cuántica,  
Carrera 30 Calle 45-03, C.P. 111321, Bogotá, Colombia*

<sup>2</sup>*Instituto de Física, Universidad de Antioquia, Medellín, A.A. 1226, Medellín, Colombia*

Using a simple fully quantum model in an effective exciton scheme that takes into account the system–environment interaction, we study the different regimes arising in a microcavity–quantum dot system. Our numerical calculations of the emission linewidth, emission energy, integrated intensity and second- and third-order correlation functions are in good qualitative agreement with reported experimental results. We show that the transition from the polariton–laser to the photon–laser regime can be defined through the critical points of both the negativity and the linear entropy of the steady state.

PACS numbers: 42.50.ct, 78.67.Hc, 42.55.sa, 03.75.Gg

The solid–state realization of Bose–Einstein Condensation (BEC) has been achieved in exciton–polariton systems [1, 2]. These quasi–bosons, arising from the strong coupling between photons and electron–hole pairs in semiconductor microcavities ( $\mu$ -C), have a high critical temperature due to their small effective mass (eight orders of magnitude smaller than hydrogen atom mass). After more than two decades of theoretical and experimental investigations, nowadays it is understood that the large occupation of the polariton ground state cannot be identified with usual thermodynamic equilibrium BEC states [1, 3, 4]. Instead, the corresponding experimentally observed regime has been called polariton laser [1, 5, 6] because of its dynamical nature and the gain in the light–emission intensity. The transition from this regime to a second one, identified with the well-known photon laser, has also been observed [5–7].

Cavity polariton systems have been studied from different theoretical perspectives. Assuming thermal equilibrium, a trial wave function that takes into account the coherence properties of both light and matter, has been able to predict multiple phase transitions [8, 9]. On the other hand, when the matter–light state is obtained from some equation of motion (mean field dynamics [10–12], master equation in multiexcitonic scheme [13], dissipative Jaynes–Cummings model [14–21]), the dynamical character of the polariton laser regime is conspicuous, and the non-Gibbsian character of the stationary state of the system is revealed. However, the elucidation of the mechanisms behind the appearance of the different observed regimes is still an open problem. Our work is a first step in this direction.

The aim of this Letter, the identification of the regimes observed in current experiments from the quantum properties of the steady state, is possible due to the simplicity of our model. Indeed, we consider a single pumped radiator interacting with a leaky mode of the electromagnetic field, ignoring collective effects. Our calculations, however, are in qualitative good agreement with

the experimental results. Moreover, we can correlate the entanglement, mixedness and the coherence functions of the steady state not only with the observed regimes but also with important physical parameters like the pumping rate and the detuning. In addition, we are able to provide a criterion to identify the “best” polariton that can be sustained by the system.

We model a quantum dot (QD) embedded in a  $\mu$ -C, as a two-level system (ground  $|G\rangle$  and excited  $|X\rangle$  states). Its interaction with a single electromagnetic mode of frequency  $\omega_C$ , in the dipole and rotating wave approximations, is described by the Hamiltonian ( $\hbar = 1$ ):

$$\hat{H} = \omega_C \hat{a}^\dagger \hat{a} + (\omega_C - \Delta) \hat{\sigma}^\dagger \hat{\sigma} + g(\hat{a} \hat{\sigma}^\dagger + \hat{a}^\dagger \hat{\sigma}). \quad (1)$$

The detuning  $\Delta$  is the difference between cavity mode and exciton energies,  $g$  is the matter–light coupling constant,  $\hat{\sigma} = |G\rangle\langle X|$  is the QD ladder operator, and  $\hat{a}^\dagger$  ( $\hat{a}$ ) is the usual creation (annihilation) operator of the cavity mode. The Hamiltonian (1) commutes with the excitation number  $\hat{N} = \hat{N}_{ph} + \hat{N}_{ex} = \hat{a}^\dagger \hat{a} + \hat{\sigma}^\dagger \hat{\sigma}$ ; hence, it only causes transitions between matter–light states of the same excitation manifold. Polaritons are defined as the energy eigenstates  $\hat{H}$ , and are explicitly given by

$$\begin{aligned} |n, +\rangle &= \sin \Phi_n |G, n\rangle + \cos \Phi_n |X, n-1\rangle \\ |n, -\rangle &= \cos \Phi_n |G, n\rangle - \sin \Phi_n |X, n-1\rangle, \end{aligned} \quad (2)$$

where  $\{|n\rangle\}$  denotes the Fock number states of the field and  $\tan 2\Phi_n = 2g\sqrt{n}/\Delta$ . We include two non-conservative processes, the loss of photons in the  $\mu$ -C ( $\kappa$ ) and the continuous pumping of excitons ( $P$ ), in the master equation for the density operator  $\hat{\rho}$  of the system

$$\begin{aligned} \frac{d\hat{\rho}}{dt} &= i[\hat{\rho}, \hat{H}] + \frac{1}{2}P(2\hat{\sigma}^\dagger \hat{\rho} \hat{\sigma} - \hat{\sigma} \hat{\sigma}^\dagger \hat{\rho} - \hat{\rho} \hat{\sigma} \hat{\sigma}^\dagger) \\ &\quad + \frac{1}{2}\kappa(2\hat{a} \hat{\rho} \hat{a}^\dagger - \hat{a}^\dagger \hat{a} \hat{\rho} - \hat{\rho} \hat{a}^\dagger \hat{a}), \end{aligned} \quad (3)$$

where we have made the Born-Markov approximation. We neglect other system–environment interaction mechanisms (e.g., spontaneous emission, dephasing, photon

pumping, polariton pumping, etc.) because their effect is either small or is already effectively contained in the master equation. If a better adjustment with the experimental results is desired those mechanisms can be included and fitted [21], but the qualitative physical image remains essentially unchanged.

The basic assumption behind our approach, which focuses on the steady state  $\hat{\rho}_{ss}$  of the equation of motion (3), is that polariton lifetime is much longer than the time required to reach the asymptotic solution [2]. The steady state  $\hat{\rho}_{ss} = \hat{\rho}(\kappa, P, g, \Delta)$  of the system, is a function of the dissipative rates  $\kappa$  and  $P$ , the matter-light coupling constant  $g$  and the detuning  $\Delta$ . In the weak-coupling regime  $g \ll P, \kappa$ , the pumping keeps the QD in its excited state while the dissipation steers the electromagnetic field to its ground state. Other states are not significantly populated because matter excitation cannot be converted into photons. On the other extreme, the ultra-strong coupling regime  $g \gg P, \kappa, \Delta$ , the long-time density matrix becomes (almost) diagonal in the basis of bare states  $|G/X, n\rangle$ . The larger the coupling  $g$  the smaller the difference of the populations of  $|G, n\rangle$  and  $|X, n-1\rangle$  ( $\propto 1/g^2$ ). The coherences  $|\rho_{GnXn-1}|$ , which decay as  $1/g$ , also vanish as the coupling  $g$  increases.

In this work we focus on the strong-coupling regime  $g \gg P, \kappa$ , in which the coherences  $\rho_{GnXn-1}$  are small, but different from zero. In resonance they are purely imaginary. For small detunings they acquire a small real part. If the detuning increases,  $\Delta \gg g$ , the matter-light interaction becomes dispersive, i.e., the energies of the matter states depend on the number of photons, and the mechanism which converts matter excitations into photons is suppressed. Thereby, large detunings correspond to a weak coupling regime. We conclude that in the regime  $|\Delta| \sim g \gg P, \kappa$ , the steady state of the system is expected to exhibit a polaritonic behavior. Unless stated otherwise, the steady state solution  $\hat{\rho}_{ss}$  of (3) is obtained for the initial condition  $\hat{\rho}(0) = |G0\rangle\langle G0|$ , and setting  $\omega_C = 1$  eV,  $g = 1$  meV and  $\kappa = 5 \times 10^{-2}$  meV, while  $\Delta$  and  $P$  are varied in ranges similar to those of current experiments [5, 6, 22].

Evidence of the spontaneous coherence build-up associated with polariton states are currently detected through the photoluminescence properties in quantum wells (QW) [1, 5, 6]. We compare our theoretical predictions in QDs with the experimental findings in QWs because: *i*) due to experimental difficulties no analogous results for QDs have been reported and *ii*) it is reasonable to assume that some of the physical mechanisms behind the exciton-polariton laser regime are the same in both cases. Additionally, the present approach may shed light on the separation of the collective effects in QWs from those of a QD single emitter.

The calculated emission linewidth, emission energy, integrated intensity and number of photons are shown in fig. 1 as a function of the pumping rate. This numerical

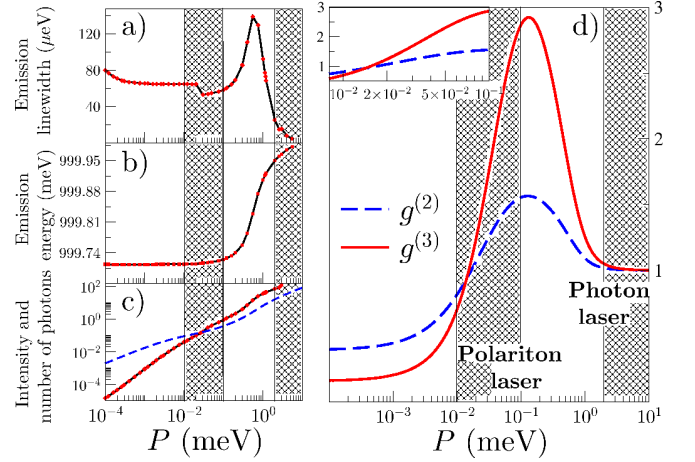


FIG. 1. (color online). (a) Emission linewidth, (b) emission energy, (c) integrated intensity (continuous line) and average number of photons (dashed line) and (d) second- and third-order correlation functions versus the incoherent exciton pumping  $P$ , for  $\kappa = 5 \times 10^{-2}$  meV and  $\Delta = 2.5$  meV. The marked regions correspond to the polariton-laser and photon-laser regimes.

calculation used the quantum regression theorem [14–16, 18] and the integrated intensity corresponds to the area under the curve of the peak associated to the transition between the polaritons in the manifolds  $n = 1$  and  $n = 2$ . The linewidth (fig.1.a) exhibits the characteristic reduction in the polariton regime, and the subsequent growth and decrease [1, 5, 6]. The emission energy blueshifts (fig.1.b) from the exciton transition frequency to the cavity mode frequency. In the polaritonic region the blueshift is smaller than observed in QWs [5, 6]. In the intermediate region,  $10^{-1}$  meV  $\lesssim P \lesssim 1$  meV, the calculated blueshift grows faster than the measured one. Despite the small slope changes in the integrated intensity as a function of  $P$  (fig.1.c) our results are consistent with the previous prediction of absence of threshold in a one-atom laser [23]. However, the nonlinearity of the model is evident in the curve of the average number of photons. Only for large values of the pumping ( $P \gtrsim 1$  meV), this curve is parallel to that of the integrated emission intensity (whose slope is approximately one).

Statistics of the emitted light can be characterized by the normalized second-  $g^{(2)}(0) = \langle \hat{a}^\dagger \hat{a}^\dagger \hat{a} \hat{a} \rangle / \langle \hat{a}^\dagger \hat{a} \rangle^2$  and third-order  $g^{(3)}(0) = \langle \hat{a}^\dagger \hat{a}^\dagger \hat{a}^\dagger \hat{a} \hat{a} \hat{a} \rangle / \langle \hat{a}^\dagger \hat{a} \rangle^3$  coherence functions, plotted in fig.(1.d). For small pumping power ( $P \lesssim 2 \times 10^{-2}$  meV)  $g^{(2)}(0), g^{(3)}(0) < 1$ , a footprint of quantum-like light, i.e. the partial state of the field is nearly a Fock state with small number of photons, as expected. Indeed, our calculations show that in this regime  $\hat{\rho}_{ss} \approx |G\rangle\langle G| \otimes \{\sin \varphi |0\rangle\langle 0| + \cos \varphi |1\rangle\langle 1|\}$ , with  $\varphi \approx 0$ . For intermediate values of the pumping ( $10^{-2}$  meV  $\lesssim P \lesssim 10^{-1}$  meV) both correlations functions monotonically grow beyond one (inset fig.1.d), as

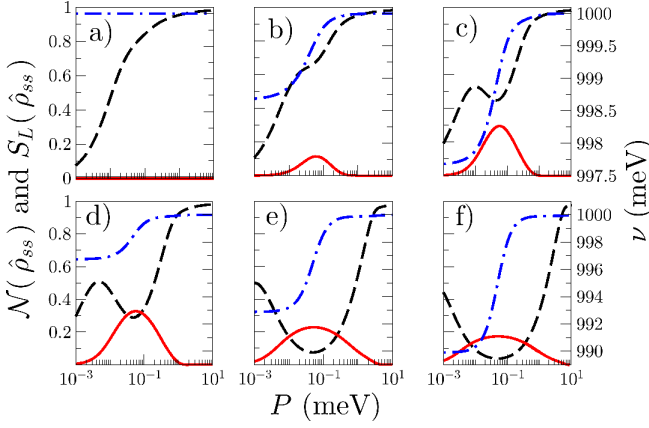


FIG. 2. (color online).  $\mathcal{N}(\hat{\rho}_{ss})$  (continuous red line),  $S_L(\hat{\rho}_{ss})$  (dashed black line) and  $\nu$  (dashed-dotted blue line) as a function of the incoherent exciton pumping  $P$ , for  $\kappa = 5 \times 10^{-2}$  meV and (a)  $\Delta = 0$ , (b)  $\Delta = 1$  meV, (c)  $\Delta = 2$  meV, (d)  $\Delta = 3$  meV, (e)  $\Delta = 7$  meV and (f)  $\Delta = 10$  meV. Note that for  $\Delta \neq 0$  the maximum of  $\mathcal{N}(\hat{\rho}_{ss})$ , the minimum of  $S_L(\hat{\rho}_{ss})$  and the inflection point of  $\nu$  coincide.

has been experimentally observed [24]. We analyze this behavior below in the text. For larger pumping rates ( $P \gtrsim 2$  meV), the state of the field becomes coherent up to third order (when  $g^{(2)}(0) = g^{(3)}(0) = 1$ ), and thus the linewidth falls (fig.1.a). In this region, the state of the field obtained by the partial trace over the excitonic degrees of freedom, has a fidelity of more than 0.99 with the random-phase coherent state  $\int_0^{2\pi} \frac{d\phi}{2\pi} |\alpha e^{i\phi}\rangle \langle \alpha e^{i\phi}|$ , where  $|\alpha e^{i\phi}\rangle$  is an usual coherent state with  $|\alpha|^2$  average number of photons. This type of state has been proposed to describe the features of a (true) photon-laser [25].

We stress that the regimes identified through the characteristics of the emitted light, mirror quantum properties of the system state. We describe those quantum properties by entanglement and mixedness of the steady state. Linear entropy and negativity are employed to quantify mixedness and matter-light entanglement, respectively. The former, defined as  $S_L(\hat{\rho}) = 1 - \text{Tr} \hat{\rho}^2$ , vanishes for pure states and is maximum for maximally mixed states. The latter is defined as  $\mathcal{N}(\hat{\rho}) = 2 \sum_{\lambda < 0} |\lambda|$ , where  $\lambda$  denotes the eigenvalues of the partial transpose of  $\hat{\rho}$  [26, 27]. Finally, searching for a relation between the energy of the system and its quantum characteristics (such as entanglement), we introduce the differential energy per excitation,  $\nu(\kappa, P) = \frac{1}{2} d \langle \hat{H} \rangle / d \langle \hat{N} \rangle$ , as a convenient measure of energy per particle. The factor of 2 in the definition of  $\nu$  has been chosen to satisfy the condition  $\nu(P \ll g, \kappa \ll \Delta) \approx \omega_C - \Delta$ . The negativity, linear entropy and the differential energy per excitation are depicted in fig. 2.

Assuming the strong-coupling regime, the formation of the polariton is hindered by two different mechanisms, which depend on the detuning. While the mixedness of

the state is large for small detuning (fig. 2.a and 2.b), matter and light decouple for large detuning (fig. 2.f). In the intermediate region  $g \lesssim |\Delta| \lesssim 10g$ , where the polariton is well defined, both mechanisms compete. The matter-light entanglement is enhanced, and the entropy of the asymptotic state of the system decreases with increasing detuning. The negativity of the steady state  $\mathcal{N}(\hat{\rho}_{ss})$  vanishes for small and large values of the pumping power, and attains a maximum at the point  $P = \kappa$  –the mid-point of the polariton-laser region.

Now, we are able to give a possible explanation of the behavior of the correlation functions in the polariton regime. The asymptotic state in the polaritonic region is a mixed entangled state which satisfies  $g^{(3)}(0) > g^{(2)}(0) > 1$ . This behavior of the correlation functions is a rather generic feature. As an example, we consider another mixed entangled state  $\hat{\rho}_{pol}(\bar{n}) = \sum_n P_n(\bar{n}) |n, +\rangle \langle n, +|$ . Since the probabilities  $P_n(\bar{n}) = e^{-\bar{n}} \bar{n}^n / (n!)$  are Poisson weights, this is a polariton coherent state. However, the reduced photon state has super-poissonian statistics, i.e., the second- and third-order coherence functions can not be expected to be unity. Hence, matter-light entanglement is a viable alternative to the standard explanation of the unexpected behavior of these functions, based on polariton-polariton and polariton-phonon interactions.

The differential energy per excitation  $\nu$  is plotted in fig. 2 as a function of  $P$  for several values of the detuning. For  $\Delta = 0$ ,  $\nu$  is independent of  $P$  and equals to the cavity mode energy, since the number of photons becomes much larger than the number of matter excitations. Our numerical results show that for  $|\Delta| \gtrsim g$ , and small ( $P < 10^{-2}$  meV) or large ( $10 \text{ meV} > P > 10^{-1}$  meV) pumping rates,  $\nu$  is almost a constant, equal to the exciton (photon) energy in the former (latter) case. The same constant values would had been obtained with the definition  $\tilde{\nu} = H/N$ . For intermediate values of  $P$ ,  $\nu$  displays an inflexion point at  $P = \kappa$ , where  $\nu = \omega_C - (\Delta/2)$  is halfway between the exciton and photon energies. Moreover, since the mean number of excitations is one, it is tempting to define  $P = \kappa$  as the condition for the “optimum” polariton. In order to quantify this idea we compare the steady state with the polariton states  $|n, \pm\rangle$  defined by (2), using the sequence of non-zero fidelities  $F_{n\pm} = \sqrt{\langle n, \pm | \hat{\rho}_{ss} | n, \pm \rangle}$ . For small values of  $P$  (fig.3.a), when  $\rho_{G_0 G_0}$  is much larger than the other populations, only  $F_{1-}$  does not vanish –however it is relatively small–. For  $P = \kappa$  (fig.3.b)  $F_{1-}$  increases up to more than 0.95, while the remaining fidelities are still small. Hence, the steady state  $\hat{\rho}_{ss}$  is quite similar to the  $\Lambda_1$ -polariton  $|1-\rangle$ . As  $P$  increases,  $F_{n\pm}$  is non-zero for larger excitation-numbers, but their values are very small.

The excitation number ( $\hat{N}$ ) symmetry associated with the Hamiltonian (1) is broken in the time evolution provided by the master equation (3), in the sense that the asymptotic state of the system cannot be labeled with a

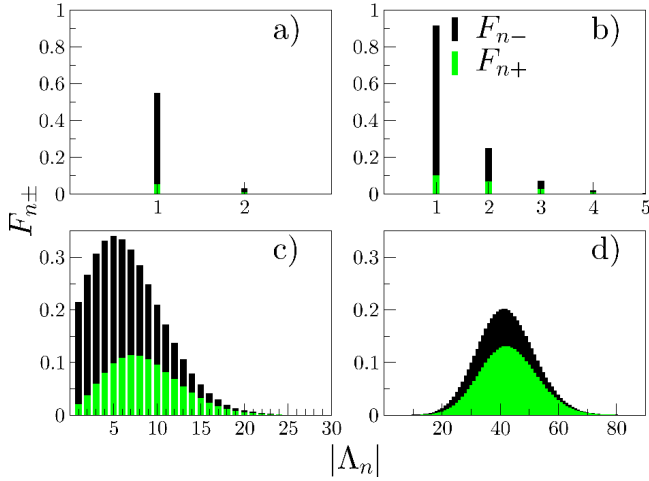


FIG. 3. (color online). Sequence of non-zero fidelities  $F_{n\pm}$  between the steady state  $\hat{\rho}_{ss}$  and the  $\Lambda_n$ -lower (black)/upper (green) polaritons  $|n, \pm\rangle$  for  $\kappa = 5 \times 10^{-2}$  meV,  $\Delta = 3$  meV and (a)  $P = 2 \times 10^{-3}$  meV, (b)  $P = 5 \times 10^{-2}$  meV, (c)  $P = 1$  meV and (d)  $P = 5$  meV.  $|\Lambda_n|$  denotes the excitation number of the polariton manifold  $\Lambda_n$ .

single eigenvalue of  $\hat{N}$ . If polariton-like behavior is actually present, restoration of the symmetry is expected. In order to account for this effect, we introduce the participation ratio  $PR = \sum_{n=0}^{\infty} P_n^2$ , where  $P_n$  is the probability to have  $n$  excitations in the asymptotic state. This quantity, which varies from zero –all excitation numbers are equiprobable– to one –only one occupied manifold–, displays a global maximum at zero pumping rate and a local maximum at  $P \approx \kappa$ , in the strong coupling regime, signaling a partial restoration of symmetry. This can be understood as a combined effect of the decrease of the mixedness of the state and the increase of its entanglement, occurring at  $P \approx \kappa$ , as discussed above (again,  $\Delta \sim g$ ).

As we have seen, the optimum polariton exhibits maximum negativity, minimum linear entropy, a local maximum of the participation ratio and an inflection point of the differential energy per excitation, provided that the system is in strong coupling. To quantify our previous qualitative arguments –which show that polaritons cannot be sustained neither for small nor for large detunings–, it is worth examining the behavior of the linear entropy and the negativity at  $P = \kappa$ , as a function of the detuning (fig.4). Three regions can be identified. In the first region,  $|\Delta| < 0.68$  meV, the negativity of the steady state is exactly zero and the linear entropy is larger than 0.72. In the second region,  $0.68 \text{ meV} < |\Delta| \lesssim 10$  meV, the linear entropy and the negativity are still significative. In the third region the dissipative polariton is very close to the Hamiltonian polariton  $|1, \pm\rangle$ , for the corresponding  $\Delta$ . Nevertheless, the dressed states (2) are virtually the bare states.

Our results might provide a guide to experiments, in

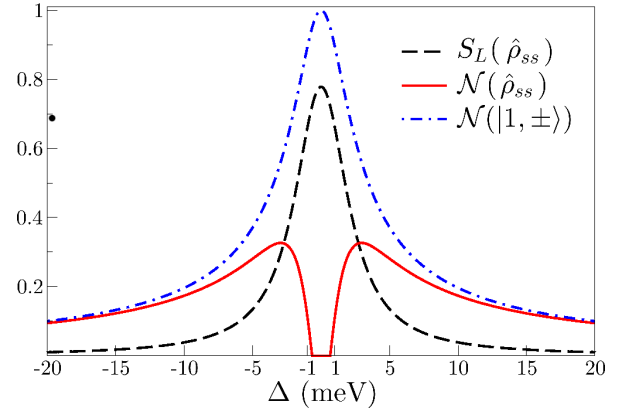


FIG. 4. (color online). Linear entropy (dashed black line) and negativity (continuous red line) of the steady state of the system  $\hat{\rho}_{ss}$ , and negativity of polaritons of the excitation manifold  $\Lambda_1$  (dashed-dotted blue line) as a function of  $\Delta$  for  $P = \kappa = 5 \times 10^{-2}$  meV.

the sense that, in the strong-coupling regime, both the pumping rate and the detuning have to be carefully adjusted. In our model, the best matter-light correlation properties occur at  $P = \kappa$  and  $\Delta \approx 3g$ , where  $\mathcal{N} \approx 0.32$  and  $S_L \approx 0.29$ . From the theoretical point of view we propose the following criterion: if the negativity rises above 0.25, close to its maximum possible value, its inflection points, as a function of the pumping power, can be used to define the polaritonic regime. When this condition is fulfilled all the quantifiers that we have examined exhibit a characteristic change. The emission energy presents a blueshift, the differential energy per excitation has an inflection point, the emission line decreases, the second- and third-order correlation functions increase beyond their value for photon coherent states, the entropy decreases and the negativity increases. With the exception of the first two, these changes can be understood as a coherence gain of the asymptotic state of the system.

We are grateful with Prof. P.S.S. Guimarães from UFMG (Brazil), Prof. J. Mahecha from UdeA (Colombia) and Dra. J. Restrepo from UAN (Colombia) for critical reading of the manuscript. The authors acknowledge partial financial support from Dirección de Investigación - Sede Bogotá, Universidad Nacional de Colombia (DIB-UNAL) under project 12584, and technical and computational support from Grupo de Óptica e Información Cuántica (GOIC-UNAL), and Grupo de Física Atómica y Molecular (GFAM-UDEA).

\* hvinckp@unal.edu.co

- [1] J. Kasprzak, M. Richard, S. Kundermann, A. Baas, P. Jeambrun, J. Keeling, F. Marchetti, M. Szymanska, R. Andre, J. Staehli, V. Savona, P. Littlewood, B. Deveaud, and L. Dang, *Nature* **443**, 409 (2006).

- [2] H. Deng, D. Press, S. Götzinger, G. S. Solomon, R. Hey, K. H. Ploog, and Y. Yamamoto, *Phys. Rev. Lett.* **97**, 146402 (2006).
- [3] H. Deng, H. Haug, and Y. Yamamoto, *Rev. Mod. Phys.* **82**, 1489 (2010).
- [4] D. Snoke, *Nature* **403**, 047401 (2006).
- [5] D. Bajoni, P. Senellart, E. Wertz, I. Sagnes, A. Miard, A. Lemaitre, and J. Bloch, *Phys. Rev. Lett.* **100**, 047401 (2008).
- [6] S. Azzini, D. Gerace, M. Galli, I. Sagnes, R. Braive, A. Lemaitre, J. Bloch, and D. Bajoni, *Appl. Phys. Lett.* **99**, 111106 (2011).
- [7] S. Christopoulos, G. von Högersthal, A. Grundy, P. Lagoudakis, A. Kavokin, J. Baumberg, G. Christmann, R. Butté, E. Felton, J.-F. Carlin, and N. Grandjean, *Phys. Rev. Lett.* **98**, 126405 (2007).
- [8] P. Littlewood, P. Eastham, J. Keeling, F. Marchetti, B. Simons, and M. Szymanska, *Journal of Physics: Condensed Matter* **16**, S3597 (2004).
- [9] K. Kamide and T. Ogawa, *Phys. Rev. Lett.* **105**, 056401 (2010).
- [10] H. Vinck-Posada, B. A. Rodriguez, and A. Gonzalez, *Physica E: Low-dimensional Systems and Nanostructures* **27**, 427 (2005).
- [11] K. G. Lagoudakis, F. Manni, B. Pietka, M. Wouters, T. C. H. Liew, V. Savona, A. V. Kavokin, R. André, and B. Deveaud-Plédran, *Phys. Rev. Lett.* **106**, 115301 (2011).
- [12] T. C. H. Liew, Y. G. Rubo, and A. V. Kavokin, *Phys. Rev. Lett.* **101**, 187401 (2008).
- [13] C. Vera, A. Cabo, and A. González, *Phys. Rev. Lett.* **102**, 126404 (2009).
- [14] J. Perea, D. Porras, and C. Tejedor, *Phys. Rev. B* **70**, 115304 (2004).
- [15] F. Laussy, E. del Valle, and C. Tejedor, *Phys. Rev. B* **79**, 235325 (2009).
- [16] E. del Valle, F. Laussy, and C. Tejedor, *Phys. Rev. B* **79**, 235326 (2009).
- [17] F. Laussy, A. Laucht, E. del Valle, J. Finley, and J. Villas-Bôas, *Phys. Rev. B* **84**, 195313 (2011).
- [18] C. Vera, N. Quesada, H. Vinck-Posada, and B. Rodríguez, *J. Phys.: Condens. Matter* **21**, 395603 (2009).
- [19] E. del Valle, F. Laussy, F. Troiani, and C. Tejedor, *Phys. Rev. B* **76**, 235317 (2007).
- [20] A. Auffèves, J.-M. Gérard, and J.-P. Poizat, *Phys. Rev. A* **79**, 053838 (2009).
- [21] A. Laucht, N. Hauke, J. M. Villas-Bôas, F. Hofbauer, G. Böhm, M. Kaniber, and J. Finley, *Phys. Rev. Lett.* **103**, 087405 (2009).
- [22] J. P. Reithmaier, G. Sek, A. Löffler, C. Hofmann, S. Kuhn, S. Reitzenstein, L. V. Keldysh, V. D. Kulakovskii, T. L. Reinecke, and A. Forchel, *Nature* **432**, 197 (2004).
- [23] P. R. Rice and H. J. Carmichael, *Phys. Rev. A* **50**, 4318 (1994).
- [24] T. Horikiri, P. Schwendimann, A. Quattropani, S. Höfling, A. Forchel, and Y. Yamamoto, *Phys. Rev. B* **81**, 033307 (2010).
- [25] K. Mølmer, *Phys. Rev. A* **55**, 3195 (1997).
- [26] K. Życzkowski, P. Horodecki, A. Sanpera, and M. Lewenstein, *Phys. Rev. A* **58**, 883 (1998).
- [27] G. Vidal and R. F. Werner, *Phys. Rev. A* **65**, 032314 (2002).